FATIGUE AND FRACTURE OF HIGH-HARDENABILITY STEELS FOR THICK-WALLED HYDROGEN PRESSURE VESSELS

San Marchi, C.[1], Bortot, P.[2], Felbaum, J.[3], Wada, Y.[4] and Ronevich, J.A.[5]
[1] Sandia National Laboratories, Livermore CA, USA, cwsanma@sandia.gov
[2] Tenaris Dalmine, Dalmine, Italy, pbortot@tenaris.com
[3] FIBA Technologies, Littleton MA, USA, JohnFelbaum@fibatech.com
[4] Japan Steel Works, Hokkaido, Japan, yoru_wada@jsw.co.jp
[5] Sandia National Laboratories, Livermore CA, USA, jaronev@sandia.gov

ABSTRACT

Stationary pressure vessels for the storage of large volumes of gaseous hydrogen at high pressure (>70 MPa) are typically manufactured from Cr-Mo steels. These steels display hydrogen-enhanced fatigue crack growth, but pressure vessels can be manufactured using defect-tolerant design methodologies. However, storage volumes are limited by the wall thickness that can be reliably manufactured for quench and tempered Cr-Mo steels, typically not more than 25-35 mm. High-hardenability steels can be manufactured with thicker walls, which enables larger diameter pressure vessels and larger storage volumes. The goal of this study is to assess the fracture and fatigue response of high hardenability, Ni-Cr-Mo pressure vessel steels for use in high-pressure hydrogen service at pressure in excess of 1000 bar. Standardized fatigue crack growth tests were performed in gaseous hydrogen at frequency of 1Hz and for R-ratios in the range of 0.1 to 0.7. Elastic-plastic fracture toughness measurements were also performed. The measured fatigue and fracture behavior is placed into the context of previous studies on fatigue and fracture of Cr-Mo steels for gaseous hydrogen.

1.0 INTRODUCTION

Hydrogen refueling infrastructure for fuel cell electric vehicles typically relies on cascade storage, namely gaseous storage in several pressure ranges to manage hydrogen storage efficiently and to facilitate the refueling of vehicles to 70 MPa. In general, these pressure vessels are manufactured from Cr-Mo steels, such as the ASME SA-372 Grade J steels. Design of the pressure vessels, however, is limited by the wall thickness of pressure vessels than can be reliably manufactured from this grade of steel, usually less than 35 mm. High hardenability pressure vessel steels, such as SA-723 steels, are an alternative to Cr-Mo steels. These steels differ primarily in the nickel content, which delays the formation of bainite during quenching, enabling the manufacture of thicker-walled pressure vessels with the desired microstructure of tempered martensite.

There is extensive engineering experience with Cr-Mo pressure vessel steels for hydrogen service. Transportable gas cylinders are typically manufactured from Cr-Mo steels, such as the 3AAX pressure vessels that are common place in laboratories throughout the US for gas distribution at pressure up to about 15 MPa. These pressure vessels are used for hydrogen as well as inert gases. Similar pressure vessels steels are used for fuel storage onboard hydrogen-fueled moving equipment, such as forklifts, but designed for service at pressure of 35 MPa. Both of these applications can claim millions of hours of operation and millions of pressure cycles with hydrogen. On the other hand, transportable gas cylinders generally do not see many pressure cycles over their lifetime. Recent work on the fatigue performance of pressure vessels for hydrogen service at pressure of 35 MPa demonstrates the structural integrity of pressure vessels designed from low-strength Cr-Mo steels [1,2]. Fatigue testing of Cr-Mo pressure vessel steels in gaseous hydrogen at 103 MPa [3,4] was motivated by the desire to certify stationary pressure vessels to the ASME Boiler and Pressure Vessel Code. Those studies provide the design basis for cascade storage in hydrogen refueling infrastructure for passenger fuel cell electric vehicles operating at pressure of 70 MPa. As the market for fuel cell electric vehicles expands, greater volumes of storage at refueling stations will be needed at lower cost. This study is motivated by the desire to advance stationary storage technology for hydrogen refueling through larger pressure vessels. This can be achieved by considering high-hardenability steels, such as Ni-Cr-Mo pressure vessel steels, for high-pressure hydrogen storage.

In this study, the fatigue and fracture behavior of several heats of high-hardenability Ni-Cr-Mo pressure vessel steels are evaluated. Additionally, this work is motivated by the need to accelerate testing methodologies for the evaluation of fatigue crack growth at low ΔK (< 10 MPa $m^{1/2}$). The measured properties are compared to Cr-Mo pressure vessel steels.

2.0 EXPERIMENTAL PROCEDURES

2.1 Materials

Several quench and tempered (Q&T) Ni-Cr-Mo pressure vessel steels were tested in this study. An ASME SA-372 Grade L steel is considered in a strength consistent with the ASME SA-372 standard (same as ASTM A372 standard). Additionally, test rings of this steel were quench and tempered to achieve a lower strength condition, significantly lower than the minimum in the SA-372 standard. The low-strength Grade L variant is referred to as Grade L-LS. A quench and tempered Ni-Cr-Mo steel was tested, which meets the SA-723 specification and the Grade 1, Class 1 designation. For this steel grade specimens were machined from a 457x40 mm (ODxWT) pressure vessel after Q&T heat treatment, therefore being very relevant from an industrial point of view. The final microstructure consisted of tempered martensite through the wall thickness. A third steel was also tested, satisfying SA-723, Grade 3 specifications for an intermediate strength level (Class 2).

The composition of these steels are provided in Table 1 and the mechanical properties are provided in Table 2.

Table 1. Composition (wt%) of the Ni-Cr-Mo pressure vessel steels reported in this study.

Designation	Fe	Ni	Cr	Mo	V	Mn	Si	C	S	P
SA-372 Grade L	Bal	1.93	0.82	0.26	nr	0.75	0.28	0.4	0.007	0.006
SA-723 Grade 1	Bal	1.5 2.25	0.80 2.00	0.20 0.40	0.20 max	0.90 max	0.35 max	0.35 max	0.015 max	0.015 max
SA-723 Grade 3	Bal	3.54	1.72	0.45	0.10	0.30	0.05	0.27	0.0008	0.005

Table 2. Mechanical properties for Ni-Cr-Mo pressure vessel steels reported in study.

Designation	Tensile Strength (MPa)	Yield Strength (MPa)	Elongation (%)
Gr L (SA-372)	1149	1053	–
Gr L-LS	873	731	–
Gr 1 Cl 1 (SA-723)	860	715	≥16
Gr 3 Cl 2 (SA-723)	978	888	15

2.2 Fatigue and Fracture Measurements

Fatigue crack growth rate testing was conducted following procedures in ASTM E647 using the compact tension (CT) geometry. The nominal geometry of the CT specimens was: thickness (B) = 12.7 mm; width (W) = 26 mm; and starter notch length = 5.2 mm. The standard designation for the orientation of the specimens is CL: loading in the circumferential direction with the crack propagating in the longitudinal direction. The specimens were side-grooved prior to precracking, resulting in a reduced thickness (B_N) of about 11.2 mm. Fatigue precracking was conducted in air at a frequency of 10 to 15 Hz to grow a crack from the starter notch to a length (a/W) of 0.28 to 0.35, where a is the crack length. A load ratio (R: equal to the minimum applied load divided by the maximum load) of 0.1 was used for precracking in all cases and the maximum stress intensity factor (K_{max}) at the conclusion of precracking was ≤ 9 MPa m$^{1/2}$.

Fatigue crack growth tests were conducted in gaseous hydrogen at a pressure of 106 MPa, following procedures described elsewhere [5] and consistent with the methods outlined in CSA CHMC1 for tests in high-pressure gaseous hydrogen (also consistent with the ASME Boiler and Pressure Vessel Code, Section VIII, Division 3, Article KD-10, except that a higher frequency is used in this study: 1 Hz compared to the specified frequency of 0.1 Hz). Briefly, the system consists of a customized high-pressure autoclave integrated to a commercial servo-hydraulic load frame. A load cell inside the autoclave is used to measure the load applied to the specimen and as the feedback signal for load control. A displacement sensor (linear variable displacement transformer) is attached to the front face of the specimen. The integrity of the environment is managed by purging the system 4 times with helium, followed by 4 purges with hydrogen at pressure of 15 MPa. The source hydrogen is 6Ns purity (99.9999%) and periodic post-test analysis of the test gas has consistently shown oxygen content less than 2 ppm and moisture less 5 ppm. Prior to initiating the fatigue loading, the specimen was typically left exposed to the test pressure for 12 to 48 hours with a small mechanical load applied to the specimen (<200 N). The soak time does not affect the response of the material, however, initial transients in the load cell readings require times in this range to reach a steady signal.

Commercial software was used to control the fatigue loading with a triangular wave form at a frequency of 1 Hz (a few short test segments were conducted at other frequencies, but a systematic study of frequency was not conducted). In general, the load ratio (R) was varied from specimen to specimen in the range of 0.1 to 0.7, but the load ratio was kept constant for each individual test specimen. In a few instances, the load ratio was changed over the course of the test in specific test segments. In general, each specimen was tested in several segments with each segment alternating between K-increasing and K-decreasing loading characteristics, where K is the applied stress intensity factor; K-increasing load cycles consisted of either constant load amplitude or a controlled positive normalized K-gradient, while K-decreasing load cycles employed a constant, negative normalized K-gradient. The segments were specified by the normalized K-gradient (C) as

$$C = (1/K)\, \mathrm{d}K/\mathrm{d}a \tag{1}$$

where K is the applied stress intensity factor and a is the crack length. Tests were conducted to show no apparent difference in the fatigue crack growth response for C values between -0.39 and +0.39 mm^{-1} for the studied conditions (e.g., frequency of 1 Hz, and positive load ratios). In a few instances, segments were conducted with $C = 0$, usually over short crack extension intervals of 1-2 mm.

The driving force for fatigue crack growth (ΔK, stress intensity factor range) is determined based on the applied load cycle and the crack length (a). The commercial control software determined the crack length from the loading compliance for every cycle to enable real-time control of the target applied peak loads (i.e., ΔK) for each successive load cycle – except when the test segment was conducted with constant load amplitude. The cycle number, crack location and ΔK, however, are recorded at fixed intervals of about 0.13 mm. The fatigue crack growth rates are determined post-test using the incremental polynomial method as described in ASTM E647 (essentially fitting a second order polynomial to a segment of data of crack length versus cycle number representing, in this case, about 0.75 mm of crack extension and evaluating the derivative of the polynomial at the middle of the crack segment for which the data is fit). Additionally, the crack lengths recorded during fatigue testing are linearly scaled to physical measurements of the crack location at the beginning and completion of fatigue testing. The physical measurements of the crack length are measured on the broken specimens using digital processing software at ten locations across the crack width, following procedures in ASTM E1820. In general, the straightness of the crack satisfies the conditions described in the standard (for the tested geometry, the minimum and maximum measured crack lengths across the crack width differ by less than 1.2 mm). In a few cases the straightness of the precrack exceeded this criterion slightly, although the cracks at the end of the fatigue test were always significantly straighter and satisfied the straightness requirements.

At the conclusion of the fatigue crack growth tests, a fracture test was conducted following the procedures of ASTM E1820 for elastic-plastic fracture toughness. Direct current potential difference was used to monitor crack position for the fracture tests, with a monotonically increasing displacement at a rate of 0.3 mm/h. Some tests were performed at slower rates by a factor of 2 or 4, but there was no significant trend with rate in the tested range. The rate of increase of K depends on the crack length, but in general, the rate of increase of the elastic component of the stress intensity factor was less than 0.01 MPa m$^{1/2}$ per second. The fracture threshold for subcritical crack growth in gaseous hydrogen is determined following standard practice for determining plane-strain fracture toughness (J_{IC}: the value of the J-integral at 0.2mm offset). Values of the fracture threshold in units of J are converted to units of K (denoted K_{JH}) for comparison with previous studies, assuming plane-strain elastic modulus of 212 GPa.

3.0 RESULTS

3.1 Fracture

The relationship between measured fracture threshold and tensile strength is consistent with reports in the literature for carbon steels (API grade pipeline steels) [5,6] and Cr-Mo pressure steels [7], as shown in the Figure 1. While the hydrogen pressure and testing rates of previous studies are somewhat different, in general, steels with a tensile strength less than 950 MPa display fracture threshold > 45 MPa m$^{1/2}$. The low-strength Ni-Cr-Mo steels (Gr L-LS and Gr 1 Cl 1) in this study are consistent with Cr-Mo steels of similar tensile strength (~860 MPa). Higher strength alloys with tensile strength > 950 MPa, on the other hand, display significantly lower fracture thresholds ≤ 20 MPa m$^{1/2}$. A steep drop in fracture threshold, however, is apparent at tensile strength of about 950 MPa: both Cr-Mo and Ni-Cr-Mo grades display fracture thresholds < 25 MPa m$^{1/2}$ above this strength limit.

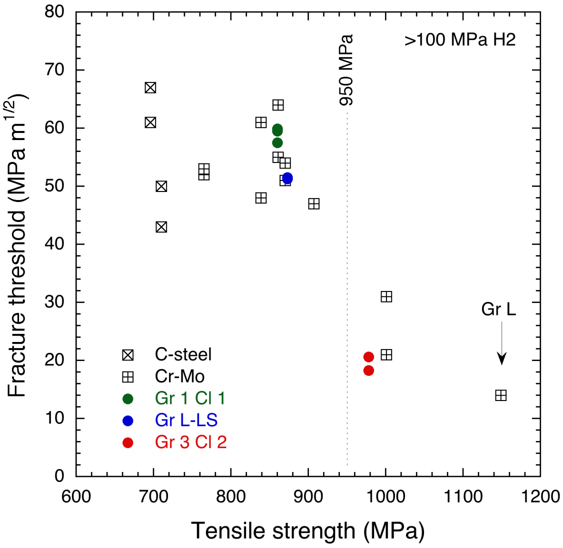

Figure 1. Fracture threshold determined from elastic-plastic fracture toughness measurements in gaseous hydrogen at pressure of 106 MPa. Carbon steel [5,6] and Cr-Mo steel [7] data from previous studies in hydrogen at pressure of 103 MPa and displacement rate of 1.5 and 3 mm/h respectively. Each data point represents an individual test.

3.2 Fatigue

The fatigue crack growth rates of all of the Ni-Cr-Mo pressure vessel steels are approximately similar in gaseous hydrogen for all the steels tested in this study. The fatigue crack growth rates at load ratio of 0.1 follow the same trend for C in the range from +0.16 to -0.39 mm^{-1}, as shown in Figure 2. Data in this plots represents five individual test specimens: two test specimens of the Gr L-LS material and one test specimen of each of the other materials. The Gr L and Gr 3 Cl 2 steels, however, appear to show an accelerated crack growth rate for $\Delta K >$ 12 MPa m$^{1/2}$. We speculate that the observed deviation from the general trend is related to acceleration in fatigue crack growth rate as the maximum stress intensity during fatigue cycling (K_{max}) approaches the threshold stress intensity factor for subcritical crack growth (K_{JH}). For the Gr L and Gr 3 Cl 2 material, the average K_{JH} is less than 20 MPa m$^{1/2}$, while for Gr L-LS and Gr 1 Cl 1, K_{max} is always substantially less than K_{JH} (which is > 50 MPa m$^{1/2}$ for both materials).

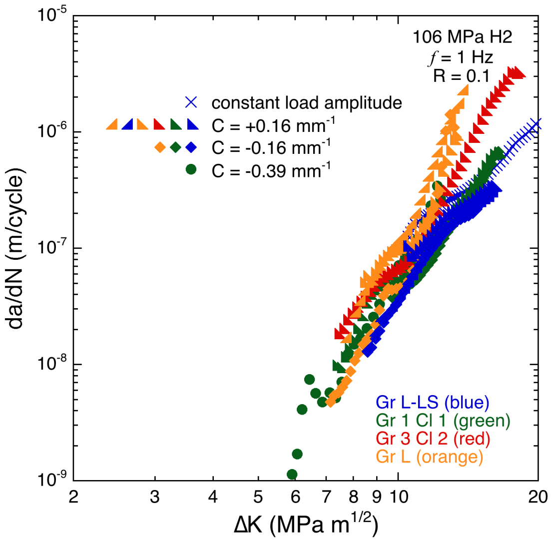

Figure 2. Fatigue crack growth rate of Ni-Cr-Mo pressure vessel steels in gaseous hydrogen at pressure of 106 MPa, with load ratio of 0.1 and frequency of 1 Hz.

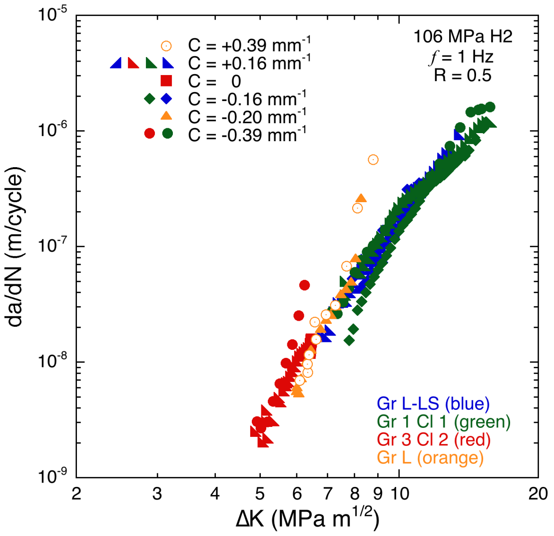

Figure 3. Fatigue crack growth rate of Ni-Cr-Mo pressure vessel steels in gaseous hydrogen at pressure of 106 MPa, with load ratio of 0.5 and frequency of 1 Hz.

The fatigue crack growth rates for load ratio of 0.5 are also consistent for all the steels in this study; data from one test specimen for each material is shown in Figure 3. As for the case of load ratio of 0.1, the Gr 3 Cl 2 steel shows a higher crack growth rate for load ratio of 0.5 when K_{max} is greater than about 13 MPa m$^{1/2}$ (Figure 3), while the Gr L steel shows transition at a slightly higher K_{max}. In general, the test-to-test variation is less for testing with load ratio of 0.5 because crack closure is less of an issue, except perhaps when the crack is very long as is the case for the few points that are below the basic trend (where $a/W \sim 0.65$); no attempt to correct for crack closure has been made in these data. It is evident from both Figure 2 and Figure 3 that K-increasing and K-decreasing tests provide similar results for C between approximately ± 0.4 mm^{-1}.

Measurement of fatigue crack growth rates for load ratio of 0.7 are challenging in high-pressure gaseous hydrogen because of the small applied load difference during the fatigue cycle and the large friction loads in the test system. The result is more uncertainty in the fatigue crack growth rates and ΔK. Despite some scatter, the fatigue crack growth rates for load ratio of 0.7 are consistent for both of the tested low-strength steels (Gr L-LS and Gr 1 Cl 1). Additionally, the range of ΔK that can be sampled is constrained when maintaining $K_{max} < K_{JH}$; for the low-strength steels K_{max} was less than about 30 MPa m$^{1/2}$ (ΔK approximately less than 9 MPa m$^{1/2}$). Fatigue crack growth tests for load ratio of 0.7 were not conducted on the high strength steels.

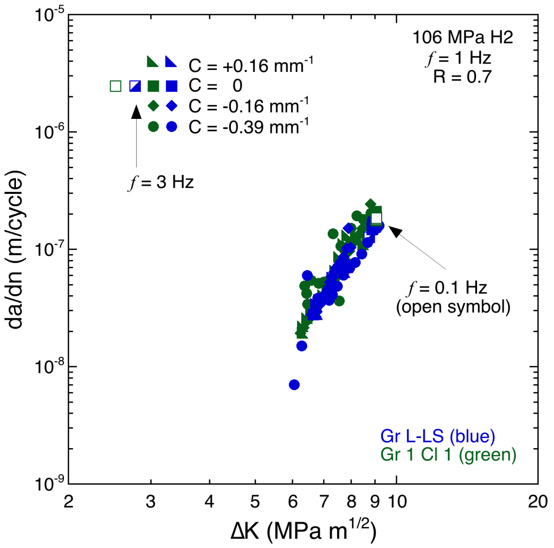

Figure 4. Fatigue crack growth rate of Ni-Cr-Mo pressure vessel steels in gaseous hydrogen at pressure of 106 MPa, for load ratio of 0.7 and frequency of 1 Hz. A few test segments were conducted at 0.1 Hz and 3 Hz, but showed no significant differences compared to test segments at 1 Hz.

4.0 DISCUSSION

In general, the fatigue crack growth rates in high-pressure gaseous hydrogen are consistent for all four Ni-Cr-Mo pressure vessel steels over a range of load ratio from 0.1 to 0.7, as shown in Figures 2 through 4. The variation in fatigue crack growth rates from test to test (or even within the same test) is a consequence of small perturbations in the determination of crack length and also crack closure (especially for long cracks). However, the composite data suggest that fatigue crack growth in high-pressure hydrogen does not depend sensitively on composition or strength of the alloy for this class of pressure vessel steels.

The fatigue crack growth rate data for Ni-Cr-Mo steels from Figures 2 through 4 can be placed into the broader context of fatigue measurements in high-pressure gaseous hydrogen by comparing to other pressure vessel steels, as in Figure 5. While the data in the literature for low ΔK is relatively limited, the fatigue crack growth rates of the high-hardenability steels in this investigation are comparable to the those reported for Cr-Mo pressure vessel steels [3,4]. One important distinction of the data for the Cr-Mo steel in Figure 5 is the lower frequency. Frequency was not systematically studied in this report, a few cursory tests (Figure 4) show no significant effect of frequency between about 0.1 and 3 Hz. While additional tests at low ΔK are needed to confirm this preliminary interpretation, the consistency of fatigue behavior between the Cr-Mo steels at 0.1 Hz [4] and the Ni-Cr-Mo steels at 1 Hz, along with other data in the literature [8], strongly suggest that for practical purposes fatigue in these steels is insensitive to frequency in the range from 0.1 to 1 Hz.

While not shown in Figure 5, the fatigue crack growth rates reported in Refs. [1,2,8] for another Cr-Mo pressure vessel steel (4130X as specified in the US Code of Federal Regulations, Title 49 Part 178 for transportable gas cylinders) are consistent with the data shown in Figure 2 for load ratio of 0.1 and Figure 5 for load ratio of 0.5. Data in the literature [5,6] for carbon steels (pipeline grades) also show consistent crack growth rates as generated here (for load ratio of 0.1 and 0.5). Collectively, these data suggest that low-strength grades of carbon steels and low-alloy steels behave similarly in hydrogen environments. In this context, low strength refers to steels with yield strength less than about 750 MPa and tensile strength less than 950 MPa. Higher strength steels, such as Gr L and Gr 3 Cl 2, also display similar fatigue crack growth behavior at low ΔK, but fatigue crack growth rates are accelerated as K_{max} approaches K_{JH}.

The effect of pressure was not explored in this study. However, the effect of hydrogen pressure on fracture thresholds of Cr-Mo pressure vessels was reported to be significant in Refs. [9]. In fatigue the emerging trends are decidedly different. For both the 4130X and the pipeline steels described above, the fatigue crack growth rates were evaluated at lower pressure: 45 MPa for the 4130X steels [1,2,8] and as low as 5 MPa for the pipeline grades [5,6]. These trends imply that, while fracture thresholds may be sensitive to hydrogen pressure, fatigue crack growth is relatively insensitive to pressure, at least for ΔK greater than about 10 MPa $m^{1/2}$ where clearly comparable data is available.

More work is needed to confirm and validate these trends, but if these trends hold, they imply that most design work for hydrogen service can utilize a set of master fatigue crack growth curves as commonly employed for structural steels in the absence of environmental effects. It should be anticipated, however, that in the fatigue threshold regime (very low ΔK), fatigue crack growth rates may be sensitive to composition and strength as well as pressure effects. For example, fatigue behavior in air is more sensitive to materials parameters (strength and composition) in the fatigue threshold regime than at crack growth rates in the Paris-Law regime (i.e., greater than about 10^{-9} m/cycle).

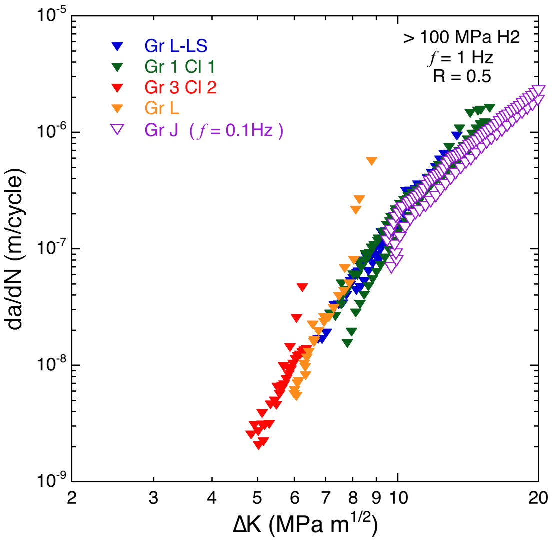

Figure 5. Comparison of fatigue crack growth rates for Ni-Cr-Mo pressure vessel steels and Ni-Cr pressure steels in high-pressure gaseous hydrogen at R = 0.5. The Ni-Cr-Mo data is from Figure 3, while the data for Cr-Mo steel represents two heats of SA-372 Grade J steel and was generated at a frequency of 0.1 Hz in hydrogen at pressure of 103 MPa from Refs. [3,4].

SUMMARY

This study focuses on fatigue crack growth rates for Ni-Cr-Mo pressure vessel steels for $\Delta K < 10$ MPa $m^{1/2}$. The effect of the normalized K-gradient (C) on fatigue was explored as a means to accelerate testing at lower crack growth rates, which represent the majority of the cycle life for growing cracks. The data in this study support an emerging description of fatigue crack growth behavior in high-pressure gaseous hydrogen for pressure vessel steels, which can be summarized as follows:

- Low-strength quench and tempered steels show fracture thresholds for subcritical crack growth greater than about 50 MPa $m^{1/2}$, while tempering to higher strength significantly reduces fracture thresholds to 20 MPa $m^{1/2}$ or less. In this context, low strength refers to yield strength less than 750 MPa and tensile strength less than 950 MPa.

- Like fatigue crack growth rates in air, fatigue crack growth rates for common pressure vessel (and pipeline) steels in high pressure gaseous hydrogen are relatively insensitive to composition and strength of the steel (at least in the limit that K_{max} is less than K_{JH}).

ACKNOWLEDGEMENTS

Sandia National Laboratories is a multimission laboratory managed and operated by National Technology and Engineering Solutions of Sandia, LLC., a wholly owned subsidiary of Honeywell International, Inc., for the U.S. Department of Energy's National Nuclear Security Administration under contract DE-NA-0003525.

REFERENCES

1. San Marchi, C., Dedrick, D.,Van Blarigan, P., Somerday, B.P. and Nibur, K.A., Pressure cycling of type 1 pressure vessels with gaseous hydrogen, in: 4th International Conference on Hydrogen Safety (ICHS4), 12-14 September 2011, San Francisco CA.
2. San Marchi, C., Harris, A., Yip, M., Somerday, B.P., Nibur, K.A., Pressure cycling of steel pressure vessel with gaseous hydrogen (PVP2012-78709), in: Proceedings of PVP-2012: ASME Pressure Vessels and Piping Division Conference, American Society of Mechanical Engineers, 15-19 July 2012, Toronto, Ontario, Canada.
3. Somerday, B.P., Nibur, K.A. and San Marchi, C., Measurement of fatigue crack growth rates for steels in hydrogen containment components, in: 3rd International Conference on Hydrogen Safety (ICHS3), September 2009, San Sebastan, Spain.
4. Somerday, B.P., San Marchi, C., Nibur, K.A., Measurement of fatigue crack growth rates for SA-372 Gr. J steel in 100 MPa hydrogen gas following Article KD-10 (PVP2013-97455), in: Proceedings of PVP-2013: ASME Pressure Vessels and Piping Division Conference, American Society of Mechanical Engineers, 14-18 July 2013, Paris, France.
5. San Marchi, C., Somerday, B.P., Nibur, K.A. , Stalheim, D.G., Boggess, T. and Jansto, S., Fracture and fatigue of commercial grade pipeline steels in gaseous hydrogen (PVP2010-25825), in: Proceedings of PVP-2010: ASME Pressure Vessels and Piping Division Conference, American Society of Mechanical Engineers, 18-22 July 2010, Bellevue WA.
6. San Marchi, C., Somerday, B.P., Nibur, K.A., Stalheim, D.G., Boggess, T., and Jansto, S., Fracture resistance and fatigue crack growth of X80 pipeline steel in gaseous hydrogen (PVP2011-57684), in: Proceedings of PVP-2011: ASME Pressure Vessels and Piping Division Conference American Society of Mechanical Engineers, July 2011, Baltimore MD.
7. Nibur, K.A., Somerday, B.P., San Marchi, C., Foulk III, J.W., Dadfarnia, M., Sofronis, P., Hayden, G.A., "Measurement and interpretation of threshold stress intensity factors for steels in high-pressure hydrogen gas", SAND2010-4633, Sandia National Laboratories, Livermore CA.
8. Nibur, K.A., San Marchi, C., Somerday, B.P., Fracture and fatigue tolerant steel pressure vessel for gaseous hydrogen (PVP2010-25827), in: Proceedings of PVP-2010: ASME Pressure Vessels and Piping Division Conference, American Society of Mechanical Engineers, 18-22 July 2010, Bellevue WA.
9. Iijima, T., Itoga, H., An, B., San Marchi, C., Somerday, B.P., Fracture properties of a Cr-Mo ferritic pressure vessel steel in high-pressure gaseous hydrogen (PVP2015-45328), in: Proceeding of PVP-2015: ASME Pressure Vessels and Pipin Division Conference, American Society of Mechanical Engineers, 19-23 July 2015, Boston MA.